Boundary element analysis of three-dimensional exponentially graded isotropic elastic solids

R. Criado*, J.E. Ortiz*, V. Mantič*, L.J. Gray† and F. París*

May 28, 2006

Abstract

A numerical implementation of the Somigliana identity in displacements for the solution of 3D elastic problems in exponentially graded isotropic solids is presented. An expression for the fundamental solution in displacements $U_{j\ell}$, was deduced by Martin et al. (*Proc. R. Soc. Lond. A*, **458**, pp. 1931–1947, 2002). This expression was recently corrected and implemented in a Galerkin indirect 3D BEM code by Criado et al. (*Int. J. for Numerical Methods in Engineering*, 2006). Starting from this expression of $U_{j\ell}$, a new expression for the fundamental solution in tractions $T_{j\ell}$ has been deduced in the present work. These quite complex expressions of the integral kernels $U_{j\ell}$ and $T_{j\ell}$ have been implemented in a collocational direct 3D BEM code. The numerical results obtained for 3D problems with known analytic solutions verify that the new expression for $T_{j\ell}$ is correct. Excellent accuracy is obtained with very coarse boundary element meshes, even for a relatively high grading of elastic properties considered.

Keywords: functionally graded materials, boundary element method, three-dimensional elasticity, Somigliana identity, fundamental solution in tractions.

1 Introduction

Functionally Graded Materials (FGMs) [1] represent a new generation of composites, having a continuous variation of apparent material properties obtained through a progressive variation of their microstructural composition. Stress concentrations appearing at material discontinuities in various applications (for example, thermal barrier coatings) can be avoided or diminished using FGMs.

The first numerical studies of FGMs have been carried out using the Finite Element Method (FEM) [2, 3, 4, 5, 6, 7] due to its capability to include, relatively easily, variation of material properties. The Boundary Element Method (BEM) [8, 9] is another technique for elastic analysis, capable of solving problems with material and geometrical discontinuities, *e.g.*, crack growth and contact, and also very suitable for flaw detection and shape optimization. Nevertheless, an adaption of BEM to non-homogeneous media is a hard task, as fundamental solutions (corresponding to concentrated loads or sources) for such media are difficult to obtain.

Fundamental solutions for heat transfer problem in non-homogeneous media have been presented in [10, 11, 12, 13, 14] and implemented in BEM codes [12, 15, 16, 17, 18]. Fundamental solutions for 2D and 3D elastic problems in exponentially graded isotropic materials have been deduced only recently in [19, 20]. These solutions have not as yet been checked computationally, to the knowledge of the present authors, which can be due to the fact that implementing them in a BEM code is far from straightforward.

In the present work the displacement fundamental solution U_{jl} corresponding to a point force in a 3D exponentially graded elastic isotropic media, developed originally in [20] and corrected in [21, 22], is employed in the form presented in [21, 22]. Moreover, a new expression of the corresponding traction fundamental solution T_{jl} is presented herein, and both functions have been implemented in a 3D collocational BEM code. To check the correctness of the kernel function expressions and to prove their suitability to be implemented in a BEM code, and also to check the overall BEM implementation, two 3D problems with known analytic solutions for exponentially graded materials have been analysed by this BEM code.

*School of Engineering, University of Seville, Camino de los Descubrimientos s/n, Sevilla, E-41092, Spain
†Computer Science and Mathematics Division, Oak Ridge National Laboratory, Oak Ridge, TN 37831-6367, USA

2 Properties of Elastic Exponentially Graded Isotropic Materials

The fourth rank tensor of elastic stiffnesses c_{ijkl} for an exponentially graded material varies according to the following law:

$$c_{ijk\ell}(\boldsymbol{x}) = C_{ijk\ell}\ \exp(2\boldsymbol{\beta}\cdot\boldsymbol{x}), \tag{1}$$

where $\boldsymbol{x}$ is a point in the material and the vector $\boldsymbol{\beta}$ defines the direction and exponential variation of grading, $\beta = \|\boldsymbol{\beta}\|$. According to (1), points situated in a plane perpendicular to $\boldsymbol{\beta}$ have the same stiffnesses, $C_{ijk\ell}$ giving the stiffnesses in the plane including the origin of coordinates.

In the case of isotropic materials, the Lamé constants λ and μ satisfy

$$c_{ijk\ell}(\boldsymbol{x}) = \lambda(\boldsymbol{x})\delta_{ij}\delta_{k\ell} + \mu(\boldsymbol{x})\left(\delta_{ik}\delta_{j\ell} + \delta_{i\ell}\delta_{jk}\right), \tag{2}$$

where δ_{ij} is Kronecker delta, and hence for exponential grading

$$\lambda(\boldsymbol{x}) = \lambda_0\ \exp(2\boldsymbol{\beta}\cdot\boldsymbol{x}) \quad \text{and} \quad \mu(\boldsymbol{x}) = \mu_0\ \exp(2\boldsymbol{\beta}\cdot\boldsymbol{x}). \tag{3}$$

Here λ_0 and μ_0 are the Lamé constants on the plane that includes the origin of coordinates. It is easy to check, that $\lambda(\boldsymbol{x})/\mu(\boldsymbol{x}) = \lambda_0/\mu_0 = 2\nu/(1-2\nu)$, ν being the (constant) Poisson ratio defined as $\nu = \lambda_0/2(\lambda_0+\mu_0)$.

3 Elastic Fundamental Solution in 3D Exponentially Graded Isotropic Materials

3.1 Displacement fundamental solution

According to [20], the displacement fundamental solution can be written as

$$\mathbf{U}(\boldsymbol{x},\boldsymbol{x}') = \exp\{-\boldsymbol{\beta}\cdot(\boldsymbol{x}+\boldsymbol{x}')\}\left\{\mathbf{U}^0(\boldsymbol{x}-\boldsymbol{x}') + \mathbf{U}^g(\boldsymbol{x}-\boldsymbol{x}')\right\}, \tag{4}$$

where $U_{j\ell}(\boldsymbol{x},\boldsymbol{x}')$ gives the j-th displacement component at $\boldsymbol{x}$ due to a unit point force acting in the ℓ-direction at point $\boldsymbol{x}'$, and $\mathbf{U}^0$ is the weakly singular Kelvin fundamental solution associated to a homogenous isotropic material defined by λ_0 and μ_0 (see [8, 9]). The so-called grading term

$$U^g_{j\ell}(\boldsymbol{x}-\boldsymbol{x}') = -\frac{1}{4\pi\mu_0 r}\left(1-\mathrm{e}^{-\beta r}\right)\delta_{j\ell} + A_{j\ell}(\boldsymbol{x}-\boldsymbol{x}') \tag{5}$$

is bounded and vanishes for $\beta = 0$, $r = \|\mathbf{r}\|$ where $\mathbf{r} = \boldsymbol{x}-\boldsymbol{x}'$.

Let an orthogonal system of coordinates $(\tilde{x}_1,\tilde{x}_2,\tilde{x}_3)$, whose origin is placed at $\boldsymbol{x}'$, be defined by the orthonormal right-handed triad $\{\boldsymbol{n},\boldsymbol{m},\hat{\boldsymbol{\beta}}\}$, where $\hat{\boldsymbol{\beta}} = (\hat{\beta}_1,\hat{\beta}_2,\hat{\beta}_3) = \boldsymbol{\beta}/\beta$, and $\boldsymbol{n}$ and $\boldsymbol{m}$ are orthonormal vectors in the plane perpendicular to $\boldsymbol{\beta}$. Let the following spherical coordinate system (r,Θ,Φ) be associated to this coordinate system:

$$\boldsymbol{r}\cdot\boldsymbol{n} = r\sin\Theta\ \cos\Phi, \quad \boldsymbol{r}\cdot\boldsymbol{m} = r\sin\Theta\ \sin\Phi \quad \boldsymbol{r}\cdot\hat{\boldsymbol{\beta}} = r\cos\Theta\ , \tag{6}$$

where $0 \le \Theta \le \pi$ and $0 \le \Phi \le 2\pi$.

According to [21, 22] the term A_{jl} is composed of the following five integrals:

$$A_{jl} = -\frac{\beta}{4\pi(1-\nu)\mu_0}\,\mathcal{I}_1 - \frac{\beta}{2\pi^2(1-\nu)\mu_0}\ (\mathcal{I}_2 - \mathcal{I}_3 + \mathcal{I}_4 - \mathcal{I}_5,)\,, \tag{7}$$

where

$$
\begin{aligned}
\mathcal{I}_1 &= \sum_{s=0}^{2}\sum_{n=0}^{2}\int_0^{\pi/2} \mathcal{R}_s^{(n)}\, \mathrm{e}^{-|k|y_s}\, I_n(Ky_s)\, \sin\theta\, \mathrm{d}\theta, && (8)\\
\mathcal{I}_2 &= \sum_{s=0}^{2}\int_{\theta_m}^{\pi/2} \mathcal{R}_s^{(0)}\, \sin\theta \int_{\eta_m}^{\pi/2} \sinh\Psi_s\, \mathrm{d}\eta\, \mathrm{d}\theta, && (9)\\
\mathcal{I}_3 &= \sum_{s=0}^{2}\int_{\theta_m}^{\pi/2} \mathcal{R}_s^{(2)}\, \sin\theta \int_{\eta_m}^{\pi/2} \sinh\Psi_s\, \cos 2\eta\, \mathrm{d}\eta\, \mathrm{d}\theta, && (10)\\
\mathcal{I}_4 &= \sum_{s=1}^{2}\int_{\theta_m}^{\pi/2} \mathcal{M}_s^{(1)}\, \sin\theta \int_{\eta_m}^{\pi/2} \cosh\Psi_s\, \sin\eta\, \mathrm{d}\eta\, \mathrm{d}\theta, && (11)\\
\mathcal{I}_5 &= \sum_{s=1}^{2}\int_{\theta_m}^{\pi/2} \tilde{\mathcal{M}}_s^{(1)}\, \mathrm{sgn}(k)\, \sin\theta \int_{\eta_m}^{\pi/2} \sinh\Psi_s\, \sin\eta\, \mathrm{d}\eta\, \mathrm{d}\theta, && (12)
\end{aligned}
$$

the extensive notation introduced in this equation being now defined.

First, $I_n(x)$ denotes the modified first kind Bessel function of order n,

$$
\begin{aligned}
I_1(Ky_s) &= \frac{2}{\pi}\int_0^{\pi/2} \sinh\left(Ky_s \sin\eta\right)\, \sin\eta\, \mathrm{d}\eta, && (13)\\
I_n(Ky_s) &= \frac{2}{\pi}\int_0^{\pi/2} \cosh\left(Ky_s \sin\eta\right)\, \cos n\eta\, \mathrm{d}\eta, \quad n = 0, 2. && (14)
\end{aligned}
$$

The integration limits θ_m and η_m $(0 \le \theta_m, \eta_m \le \frac{\pi}{2})$ are defined by

$$
\theta_m(\Theta) = \left|\tfrac{1}{2}\pi - \Theta\right|, \qquad |k(r,\Theta,\theta)| = K(r,\Theta,\theta)\sin\eta_m(\Theta,\theta), \tag{15}
$$

where $k(r,\Theta,\theta) = \beta r\cos\theta\,\cos\Theta$ and $K(r,\Theta,\theta) = \beta r\sin\theta\,\sin\Theta$, and the range of θ guarantees that η_m is well defined. The argument of the hyperbolic functions is

$$
\Psi_s(r,\Theta,\theta,\eta) = K(r,\Theta,\theta)y_s(\theta)\left(\sin\eta_m(\Theta,\theta) - \sin\eta\right), \tag{16}
$$

where the functions y_s are given by

$$
y_0 = 1, \quad y_1(\theta) = \sqrt{q(\theta) + \sqrt{q^2(\theta) - 1}}, \quad y_2(\theta) = \sqrt{q(\theta) - \sqrt{q^2(\theta) - 1}}\,, \tag{17}
$$

with $q(\theta) \ge 1$ defined as

$$
q(\theta) = 1 + \frac{2\nu}{1-\nu}\sin^2(\theta). \tag{18}
$$

The functions $\mathcal{R}_s^{(n)}$ and $\mathcal{M}_s^{(n)}$ are given by

$$
\mathcal{R}_s^{(0)} = \mathcal{M}_s^{(0)}, \qquad \mathcal{R}_s^{(2)} = -\mathcal{M}_s^{(2)}, \quad s = 0, 1, 2, \tag{19}
$$

$$
\mathcal{R}_s^{(1)} = -\left(\mathcal{M}_s^{(1)} + \widetilde{\mathcal{M}}_s^{(1)}\,\mathrm{sgn}(k)\right), \quad s = 1, 2, \tag{20}
$$

$$
\mathcal{M}_0^{(n)} = \frac{f_n(1)}{2\,D(1)}, \qquad \mathcal{M}_s^{(n)} = \frac{f_n(y_s)}{(1 - y_s^2)\,D'(y_s)}, \quad n = 0, 2 \quad \text{and} \quad s = 1, 2, \tag{21}
$$

$$
\mathcal{M}_s^{(1)} = \frac{f_1(y_s)}{D'(y_s)}, \qquad \widetilde{\mathcal{M}}_s^{(1)} = \frac{\tilde{f}_1(y_s)}{D'(y_s)}, \quad s = 1, 2, \tag{22}
$$

while the functions f_i are defined by

$$
\begin{aligned}
f_0(x) &= \tfrac{1}{2}\{8\nu x^4 - (-x^2+1)(-2x^2q+1)\}(n_j n_\ell + m_j m_\ell)\sin^2\theta && (23)\\
&\quad + \left\{8\nu x^4 \sin^2\theta + (-x^2+1)[-x^2 - (-2x^2q+1)\cos^2\theta]\right\}\hat{\beta}_j\hat{\beta}_\ell, && (24)\\
f_1(x) &= x^3(4\nu - 1)(s_j\hat{\beta}_\ell - \hat{\beta}_j s_\ell)\sin\theta, && (25)\\
\tilde{f}_1(x) &= -\tfrac{1}{2}(s_j\hat{\beta}_\ell + \hat{\beta}_j s_\ell)(-2x^2q+1)\sin 2\theta, && (26)\\
f_2(x) &= -\tfrac{1}{2}[8\nu x^4 - (-x^2+1)(-2x^2q+1)]\left\{n_j(n_\ell\cos 2\Phi + m_\ell\sin 2\Phi)\right. && (27)\\
&\quad \left. + m_j(n_\ell\sin 2\Phi - m_\ell\cos 2\Phi)\right\}\sin^2\theta, && (28)\\
s_j(\Phi) &= n_j\cos\Phi + m_j\sin\Phi, && (29)
\end{aligned}
$$

and the polynomials $D(x)$ and $D'(x)$ by

$$D(x) = x^4 - 2x^2 q + 1 \quad \text{and} \quad D'(x) = -4x^3 + 4xq \; . \tag{30}$$

Notice that $D'(x)$ is not the derivative of $D(x)$.

A discussion of the properties of the fundamental solution U_{jl} and some aspects of the above expression, together with recommendations for its numerical evaluation can be found in [21, 22].

3.2 Traction fundamental solution

The direct boundary integral equation for surface displacement requires the displacement fundamental solution, and the corresponding traction fundamental solution. The starting point in the evaluation of tractions in an exponentially graded material due to a unit point force is the differentiation of the fundamental solution in displacements U_{jl}. These derivatives are used to determine the corresponding strains, and then employing the constitutive law with the tensor of elastic stiffnesses given in (2-3), the corresponding stresses can be obtained.

Differentiation of (4) yields

$$\frac{\partial U_{j\ell}}{\partial x_k}(\boldsymbol{x},\boldsymbol{x}') = \exp\left(-\boldsymbol{\beta}\cdot(\boldsymbol{x}+\boldsymbol{x}')\right)\left(\frac{\partial U^0_{j\ell}}{\partial x_k}(\boldsymbol{x}-\boldsymbol{x}') + \frac{\partial U^g_{j\ell}}{\partial x_k}(\boldsymbol{x}-\boldsymbol{x}')\right) - \beta_k U_{j\ell}(\boldsymbol{x},\boldsymbol{x}') \; . \tag{31}$$

Although the derivative of $U^0_{j\ell}$ is strongly singular, this term eventually produces the Kelvin traction kernel for a homogeneous material; the expressions can be found in [8, 9]. The derivative of $U^g_{j\ell}$ is weakly singular and can be expressed, in view of (5), as

$$\frac{\partial U^g_{j\ell}}{\partial x_k}(\boldsymbol{x}-\boldsymbol{x}') = -\frac{\delta_{j\ell}}{4\pi\mu_0}\left\{\frac{\mathrm{e}^{-\beta\, r}(\beta\, r_{,k})}{r} - \frac{(1-\mathrm{e}^{-\beta\, r})r_{,k}}{r^2}\right\} + \frac{\partial A_{j\ell}}{\partial x_k}(\boldsymbol{x}-\boldsymbol{x}') \; , \tag{32}$$

where the derivative of A_{jl} is, according to (7), decomposed into the sum of the derivatives of the integrals $\mathcal{I}_i$

$$\frac{\partial A_{jl}}{\partial x_k}(\boldsymbol{x}-\boldsymbol{x}') = -\frac{\beta}{4\pi(1-\nu)\mu_0}\frac{\partial \mathcal{I}_1}{\partial x_k} - \frac{\beta}{2\pi^2(1-\nu)\mu_0}\left(\frac{\partial \mathcal{I}_2}{\partial x_k} - \frac{\partial \mathcal{I}_3}{\partial x_k} + \frac{\partial \mathcal{I}_4}{\partial x_k} - \frac{\partial \mathcal{I}_5}{\partial x_k}\right) \; . \tag{33}$$

Note that the weakly singular character of $\partial U^g_{j\ell}/\partial x_k$ directly follows from the boundedness of $U^g_{j\ell}$ and the Gauss divergence theorem.

When differentiating $\mathcal{I}_i$ ($i = 2,\ldots,5$), involving double integrals with respect to η and θ, it should be taken into account that while their superior limits are constant, their inferior limits are varying with the positions of the field and source points, $\boldsymbol{x}$ and $\boldsymbol{x}'$, as follows:

- Inferior limit of the integral in θ: $\theta_m = \theta_m(\boldsymbol{x},\boldsymbol{x}')$,
- Inferior limit of the integral in η: $\eta_m = \eta_m(\boldsymbol{x},\boldsymbol{x}',\theta)$.

Thus, derivatives of these doubles integrals are evaluated by applying the following rule twice:

$$\frac{d}{dx}\int_{A(x)}^{B} f(x,t)\mathrm{d}t = \int_{A(x)}^{B} \frac{\partial f(x,t)}{\partial x}\mathrm{d}t - f(x,A(x))\frac{dA}{dx}. \tag{34}$$

By also taking into account that $\eta_m(\theta=\theta_m) = \pi/2$ and consequently $\Psi_s(\eta=\eta_m) = 0$, see [21], the following expressions are obtained after some algebraic manipulations:

$$\frac{\partial \mathcal{I}_1}{\partial x_k} = \sum_{s=0}^{2}\sum_{n=0}^{2}\int_0^{\pi/2} \mathrm{e}^{-|k|y_s}\,\sin\theta\left\{\frac{\partial \mathcal{R}_s^{(n)}}{\partial x_k}\,I_n(Ky_s) + \mathcal{R}_s^{(n)}\left(-y_s\,\frac{\partial |k|}{\partial x_k}I_n(Ky_s) + \frac{\partial I_n(Ky_s)}{\partial x_k}\right)\right\}\mathrm{d}\theta \tag{35}$$

$$\frac{\partial \mathcal{I}_2}{\partial x_k} = \sum_{s=0}^{2}\int_{\theta_m}^{\pi/2}\sin\theta\left\{\frac{\partial \mathcal{R}_s^{(0)}}{\partial x_k}\int_{\eta_m}^{\pi/2}\sinh\Psi_s\,\mathrm{d}\eta + \mathcal{R}_s^{(0)}\left\{\int_{\eta_m}^{\pi/2}\cosh\Psi_s\,\frac{\partial\Psi_s}{\partial x_k}\mathrm{d}\eta\right\}\right\}\mathrm{d}\theta \tag{36}$$

$$\frac{\partial \mathcal{I}_3}{\partial x_k} = \sum_{s=0}^{2}\int_{\theta_m}^{\pi/2}\sin\theta\left\{\frac{\partial \mathcal{R}_s^{(2)}}{\partial x_k}\int_{\eta_m}^{\pi/2}\sinh\Psi_s\,\cos 2\eta\mathrm{d}\eta + \mathcal{R}_s^{(2)}\left\{\int_{\eta_m}^{\pi/2}\cosh\Psi_s\cos 2\eta\,\frac{\partial\Psi_s}{\partial x_k}\mathrm{d}\eta\right\}\right\}\mathrm{d}\theta \tag{37}$$

$$\frac{\partial \mathcal{I}_4}{\partial x_k} = \sum_{s=1}^{2}\int_{\theta_m}^{\pi/2}\sin\theta\left\{\left(\frac{\partial \mathcal{M}_s^{(1)}}{\partial x_k}\right)\int_{\eta_m}^{\pi/2}\cosh\Psi_s\,\sin\eta\mathrm{d}\eta + \mathcal{M}_s^{(1)}\left\{\int_{\eta_m}^{\pi/2}\sinh\Psi_s\sin\eta\,\frac{\partial\Psi_s}{\partial x_k}\mathrm{d}\eta - \frac{\partial\eta_m}{\partial x_k}\,\sin\eta_m\right\}\right\}\mathrm{d}\theta \tag{38}$$

$$\frac{\partial \mathcal{I}_5}{\partial x_k} = \sum_{s=1}^{2}\int_{\theta_m}^{\pi/2}\sin\theta\left\{\left(\frac{\partial \tilde{\mathcal{M}}_s^{(1)}}{\partial x_k}\mathrm{sgn}(k)\right)\int_{\eta_m}^{\pi/2}\sinh\Psi_s\,\sin\eta\mathrm{d}\eta + \tilde{\mathcal{M}}_s^{(1)}\,\mathrm{sgn}(k)\left\{\int_{\eta_m}^{\pi/2}\cosh\Psi_s\sin\eta\,\frac{\partial\Psi_s}{\partial x_k}\mathrm{d}\eta\right\}\right\}\mathrm{d}\theta \tag{39}$$

where

$$\frac{\partial \mathcal{R}_s^{(n)}}{\partial x_k} = 0, \quad n=0 \text{ and } n=1 \text{ with } s=0, \tag{40}$$

$$= -\frac{\partial \mathcal{M}_s^{(1)}}{\partial x_k} - \frac{\partial \widetilde{\mathcal{M}}_s^{(1)}}{\partial x_k}\mathrm{sgn}(k), \quad n=1 \text{ with } s=1,2, \tag{41}$$

$$= -\frac{\partial \mathcal{M}_s^{(2)}}{\partial x_k}, \quad n=2, \tag{42}$$

$$\frac{\partial\Psi_s}{\partial x_k} = \frac{\partial K}{\partial x_k}y_s(\sin\eta_m - \sin\eta) + K\,y_s\,\cos\eta_m\,\frac{\partial\eta_m}{\partial x_k}, \tag{43}$$

$$\frac{\partial I_n}{\partial x_k} = \frac{2}{\pi(-1)^{n/2}}\int_0^{\pi/2}\cos(n\eta)\,\sinh(K\,y_s\sin\eta)\frac{\partial K}{\partial x_k}y_s\,\sin\eta\mathrm{d}\eta, \quad n=0,2, \tag{44}$$

$$= \frac{2}{\pi}\int_0^{\pi/2}\sin(\eta)\,\cosh(K\,y_s\sin\eta)\frac{\partial K}{\partial x_k}y_s\,\sin\eta\mathrm{d}\eta, \quad n=1. \tag{45}$$

The derivative of η_m is expressed as

$$\frac{\partial\eta_m}{\partial x_k} = \frac{1}{K\cos\eta_m}\left\{\frac{\partial|k|}{\partial x_k} - \sin\eta_m\frac{\partial K}{\partial x_k}\right\}, \tag{46}$$

where

$$\frac{\partial k}{\partial x_k} = \beta\,\left(\frac{\partial r}{\partial x_k}\cos\theta\cos\Theta + r\cos\theta\frac{\partial\cos\Theta}{\partial x_k}\right), \tag{47}$$

$$\frac{\partial K}{\partial x_k} = \beta\,\left(\frac{\partial r}{\partial x_k}\sin\theta\sin\Theta + r\sin\theta\frac{\partial\sin\Theta}{\partial x_k}\right). \tag{48}$$

The derivatives of $\mathcal{M}_s^{(n)}$ and $\widetilde{\mathcal{M}}_s^{(n)}$ appearing in the above expressions are given by:

$$\frac{\partial \mathcal{M}_s^{(n)}}{\partial x_k} = 0, \quad n=0, \tag{49}$$

$$= \frac{1}{D'(y_s)}\frac{\partial f_1}{\partial x_k}(y_s), \quad n=1, \tag{50}$$

$$= \frac{1}{D(1)}\frac{\partial f_2}{\partial x_k}(1), \quad n=2 \text{ with } s=0, \tag{51}$$

$$= \frac{1}{(1-{y_s}^2)\,D'(1)}\frac{\partial f_2}{\partial x_k}(1), \quad n=2 \text{ with } s=1,2, \tag{52}$$

$$\frac{\partial \widetilde{\mathcal{M}}_s^{(1)}}{\partial x_k} = \frac{1}{D'(y_s)}\frac{\partial \tilde{f}_1}{\partial x_k}(y_s), \tag{53}$$

where

$$\frac{\partial f_1}{\partial x_k}(x) = x^3(4\nu - 1)\left(\frac{\partial s_j}{\partial x_k}\hat{\beta}_l - \frac{\partial s_l}{\partial x_k}\hat{\beta}_j\right)\sin\theta \tag{54}$$

$$\frac{\partial f_2}{\partial x_k}(x) = -0.5\left[8\nu x^4 - (-x^2+1)(-2x^2q+1)\right]\Bigg\{n_j\left(n_l\frac{\partial\cos 2\Phi}{\partial x_k} + m_l\frac{\partial\sin 2\Phi}{\partial x_k}\right) \tag{55}$$

$$+ m_j\left(n_l\frac{\partial\sin 2\Phi}{\partial x_k} - m_l\frac{\partial\cos 2\Phi}{\partial x_k}\right)\Bigg\}\sin^2\theta \tag{56}$$

$$\frac{\partial\tilde{f}_1}{\partial x_k}(x) = -0.5\left(\frac{\partial s_j}{\partial x_k}\hat{\beta}_l + \frac{\partial s_l}{\partial x_k}\hat{\beta}_j\right)(-2x^2q+1)\sin 2\theta\ . \tag{57}$$

$$\tag{58}$$

Finally,

$$\frac{\partial s_j}{\partial x_k} = n_j\,\frac{\partial\cos\Phi}{\partial x_k} + m_j\,\frac{\partial\sin\Phi}{\partial x_k} \tag{59}$$

$$\frac{\partial}{\partial x_k} = \frac{\partial}{\partial\tilde{x}_j}\frac{\partial\tilde{x}_j}{\partial x_k} = L_{jk}\frac{\partial}{\partial\tilde{x}_j}, \tag{60}$$

where $L_{1k} = n_k$, $L_{2k} = m_k$, $L_{3k} = \hat{\beta}_k$, and

$$\frac{\partial\cos\Theta}{\partial\tilde{x}_j} = \frac{\delta_{j3}}{r} - \frac{r_3}{r^2}\,\frac{\partial r}{\partial\tilde{x}_j}\ , \tag{61}$$

$$\frac{\partial\sin\Theta}{\partial\tilde{x}_j} = \frac{1}{r\sqrt{r^2-r_3^2}}\left(r\frac{\partial r}{\partial\tilde{x}_j} - r_3\,\delta_{j3}\right) - \frac{\sqrt{r^2-r_3^2}}{r^2}\,\frac{\partial r}{\partial\tilde{x}_j}\ , \tag{62}$$

$$\frac{\partial\cos\Phi}{\partial\tilde{x}_j} = \frac{\delta_{j1}}{\sqrt{r^2-r_3^2}} - \frac{r_1}{(r^2-r_3^2)^{3/2}}\left(r\frac{\partial r}{\partial\tilde{x}_j} - r_3\,\delta_{j3}\right)\ , \tag{63}$$

$$\frac{\partial\sin\Phi}{\partial\tilde{x}_j} = \frac{\delta_{j2}}{\sqrt{r^2-r_3^2}} - \frac{r_1}{(r^2-r_3^2)^{3/2}}\left(r\frac{\partial r}{\partial\tilde{x}_j} - r_3\,\delta_{j3}\right)\ . \tag{64}$$

The strains $E_{ij\ell}(\boldsymbol{x},\boldsymbol{x}')$ associated with the fundamental solution in displacements $U_{j\ell}(\boldsymbol{x},\boldsymbol{x}')$ given by

$$E_{ij\ell}(\boldsymbol{x},\boldsymbol{x}') = \frac{1}{2}\left(\frac{\partial U_{i\ell}}{\partial x_j}(\boldsymbol{x},\boldsymbol{x}') + \frac{\partial U_{j\ell}}{\partial x_i}(\boldsymbol{x},\boldsymbol{x}')\right)\ , \tag{65}$$

and thus incorporating the constitutive law defining the elastic stiffnesses (2-3), yields the corresponding stresses

$$\Sigma_{ij\ell} = 2\mu(\boldsymbol{x})E_{ij\ell}(\boldsymbol{x},\boldsymbol{x}') + \lambda(\boldsymbol{x})E_{kk\ell}(\boldsymbol{x},\boldsymbol{x}')\delta_{ij}\ . \tag{66}$$

Then, substituting (65) into (66) and using (31) yields

$$\Sigma_{ij\ell}(\boldsymbol{x}-\boldsymbol{x}') = \exp\left(\boldsymbol{\beta}\cdot(\boldsymbol{x}-\boldsymbol{x}')\right)\left(\Sigma^0_{ij\ell}(\boldsymbol{x}-\boldsymbol{x}') + \Sigma^g_{ij\ell}(\boldsymbol{x}-\boldsymbol{x}')\right)\ , \tag{67}$$

where the strongly singular term $\Sigma^0_{ij\ell}(\boldsymbol{x}-\boldsymbol{x}')$ represents the stress tensor σ_{ij} at $\boldsymbol{x}$ originated by a unit point force in direction ℓ at $\boldsymbol{x}'$ in the homogeneous elastic isotropic material having Lamé constants μ_0 and λ_0 (see [8, 9]). The weakly singular grading term $\Sigma^g_{ij\ell}(\boldsymbol{x}-\boldsymbol{x}')$ is expressed as:

$$\begin{aligned}\Sigma^g_{ij\ell}(\boldsymbol{x}-\boldsymbol{x}') \quad &= \quad \mu_0\left(\frac{\partial U^g_{i\ell}}{\partial x_j} + \frac{\partial U^g_{j\ell}}{\partial x_i} - \beta_i\left(U^0_{j\ell} + U^g_{j\ell}\right) - \beta_j\left(U^0_{i\ell} + U^g_{i\ell}\right)\right)\\ &\quad + \lambda_0\left(\frac{\partial U^g_{k\ell}}{\partial x_k} - \beta_k\left(U^0_{k\ell} + U^g_{k\ell}\right)\right)\delta_{ij}\ .\end{aligned} \tag{68}$$

Finally the corresponding traction vector $T_{i\ell}(\boldsymbol{x},\boldsymbol{x}')$, associated with the unit outward normal vector $\mathbf{n}(\boldsymbol{x})$, is obtained from $\Sigma_{ij\ell}(\boldsymbol{x}-\boldsymbol{x}')$ by the Cauchy lemma:

$$T_{i\ell}(\boldsymbol{x},\boldsymbol{x}') = \Sigma_{ij\ell}(\boldsymbol{x}-\boldsymbol{x}')\,n_j(\boldsymbol{x}) \tag{69}$$

$$= \exp\left(\boldsymbol{\beta}\cdot(\boldsymbol{x}-\boldsymbol{x}')\right)\left(T^0_{i\ell}(\boldsymbol{x},\boldsymbol{x}') + T^g_{i\ell}(\boldsymbol{x},\boldsymbol{x}')\right)\ , \tag{70}$$

where, as for the stress, $T^0_{i\ell}(\boldsymbol{x},\boldsymbol{x}')$ represents the well-known strongly singular fundamental solution in tractions for a homogeneous material (parameters μ_0 and λ_0) (see [8, 9]), and $T^g_{i\ell}(\boldsymbol{x},\boldsymbol{x}')$ is the weakly singular grading term obtained from $\Sigma^g_{ij\ell}(\boldsymbol{x}-\boldsymbol{x}')$, $T^g_{i\ell}(\boldsymbol{x},\boldsymbol{x}') = \Sigma^g_{ij\ell}(\boldsymbol{x}-\boldsymbol{x}')\,n_j(\boldsymbol{x})$.

4 Boundary Element Method

The boundary integral formulation for an isotropic, exponentially graded body Ω with (Lipschitz and piecewise smooth) boundary $\partial\Omega = \Gamma$ will be briefly discussed in this section. The derivation follows the standard procedures for a homogeneous material [8, 9]. Starting from the 2nd Betti Theorem of reciprocity of work for a graded material, one can derive the corresponding Somigliana identity,

$$C_{i\ell}(\boldsymbol{x}')u_i(\boldsymbol{x}') + \fint_{\Gamma} T_{i\ell}(\boldsymbol{x},\boldsymbol{x}')u_i(\boldsymbol{x})dS(\boldsymbol{x}) = \int_{\Gamma} U_{i\ell}(\boldsymbol{x},\boldsymbol{x}')t_i(\boldsymbol{x})dS(\boldsymbol{x}) \ , \tag{71}$$

expressing the displacements $u_i(\boldsymbol{x}')$ at a domain or boundary point $\boldsymbol{x}' \in \Omega \cup \Gamma$ in terms of the boundary displacements $u_i(\boldsymbol{x})$ and tractions $t_i(\boldsymbol{x})$, $\boldsymbol{x} \in \Gamma$. The strongly singular traction kernel integral is evaluated in the Cauchy principal value sense, and

$$C_{i\ell}(\boldsymbol{x}') = \lim_{\varepsilon\to 0_+} \int_{S_\varepsilon(\boldsymbol{x}')\cap\Omega} T_{i\ell}(\boldsymbol{x},\boldsymbol{x}')dS(\boldsymbol{x}) \tag{72}$$

is the coefficient tensor of the free term, $S_\varepsilon(\boldsymbol{x}')$ being a spherical surface of radius ε centered at $\boldsymbol{x}'$. It is important to note that, despite the complexity of the $T_{i\ell}$ kernel expression, this evaluation is not a problem. The weakly singular grading term and the exponential coefficient in (70) will play no role in the limit procedure in (72). Thus, the value of $C_{i\ell}$ in (72) coincides with the value of $C_{i\ell}$ for the homogeneous isotropic material whose properties are defined by the Lamé constants λ_0 and μ_0, *i.e.*,

$$C_{i\ell}(\boldsymbol{x}') = \lim_{\varepsilon\to 0_+} \int_{S_\varepsilon(\boldsymbol{x}')\cap\Omega} T^0_{i\ell}(\boldsymbol{x},\boldsymbol{x}')dS(\boldsymbol{x}). \tag{73}$$

Hence, $C_{i\ell}(\boldsymbol{x}') = \delta_{i\ell}$ for $\boldsymbol{x}' \in \Omega$, $C_{i\ell}(\boldsymbol{x}') = \frac{1}{2}\delta_{i\ell}$ for $\boldsymbol{x}' \in \Gamma$ situated at a smooth part of Γ, and for an edge or corner point of Γ, $C_{i\ell}(\boldsymbol{x}')$ is given by the size, shape and spatial orientation of the interior solid angle at $\boldsymbol{x}'$. A general explicit analytic expression of the symmetric tensor $C_{i\ell}(\boldsymbol{x}')$ in terms of the unit vectors tangential to the boundary edges and the unit outward normal vectors to the boundary surfaces at $\boldsymbol{x}'$ can be found in [23].

The numerical implementation of (71) in this work employs standard approximation techniques. A collocation approximation based upon a nine-node continuous quadrilateral quadratic isoparametric element is employed to interpolate the boundary and the boundary functions. The evaluation of regular integrals is accomplished by Gaussian quadrature with 8×8 integration points, whereas an adaptive element subdivision following the procedure developed in [24] is utilized for nearly singular integrals. A standard polar coordinate transformation [24] is employed to handle the weakly singular integrals involving the kernel $U_{i\ell}$, and the rigid body motion procedure is invoked for evaluating the sum of the coefficient tensor of the free term $C_{i\ell}$ and the Cauchy principal value integral with the kernel $T_{i\ell}$.

5 Numerical Results

The expression for the $T_{i\ell}(\boldsymbol{x},\boldsymbol{x}')$ kernel is clearly quite complicated, and thus it is necessary to verify that these formulas and their numerical implementation are correct. This is accomplished in this section using two relatively simple problems having known exact solutions.

Consider the cube $\Omega = (0,\ell)^3$ wherein the material is exponentially graded in x_3-direction. The grading coefficient β in the numerical tests will be chosen as $(\ln 2)/\ell$ or $(\ln 7)/\ell$; thus, the Young modulus increases in the x_3-direction 4 or 49 times, respectively, *i.e.*, $E(x_3 = \ell)/E_0 = 4$ or 49, where $E_0 = E(x_3 = 0)$. In both test problems, symmetry boundary conditions are imposed on the three faces coincident with the coordinate planes: $x_1 = 0$, $x_2 = 0$ and $x_3 = 0$. Elastic solutions in this cube having different loads and different Poisson ratios ν will be studied using three very coarse meshes, denoted as A, B and C. Mesh A has one element per face, and therefore 6 total elements, while the meshes B and C are obtained by dividing each element of mesh A parallel to the x_3-direction into 2 and 3 uniform elements, respectively. This results in a total of 10 and 14 elements. These meshes are shown in Figure 1, together with the above symmetry boundary conditions.

The percentages of the normalized error in stresses and displacements will be computed as

$$\%Err(\sigma_{ij}) = \frac{\sigma_{ij}^{\rm BEM} - \sigma_{ij}^{\rm anal.}}{\sigma_0} \times 100, \qquad \%Err(u_i) = \frac{u_i^{\rm BEM} - u_i^{\rm anal.}}{\max\ u_i^{\rm anal.}} \times 100 \ , \tag{74}$$

where σ_0 is a nominal stress involved in the definition of each problem.

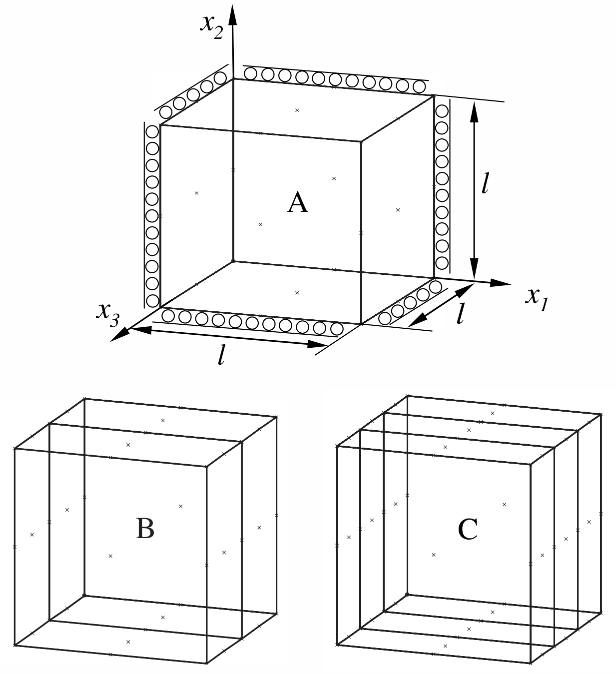

Figure 1: Three BEM discretizations of cube (A, B and C) using 6, 10 and 14 elements, respectively.

Table 1: Normalized errors in σ_{33} at the plane $x_3 = 0$. Grading coefficient $\beta = (\ln 2)/\ell$. Meshes A, B and C.

		Normalized error (%)		
Node	Coordinates	A	B	C
1	(0, 0, 0)	-0.9931	-0.2070	0.0149
2	(0.5ℓ, 0, 0)	0.0311	-0.0080	0.0123
3	(ℓ, 0, 0)	-0.4273	-0.1961	-0.1951
4	(0, 0.5ℓ, 0)	0.0311	-0.0078	0.0128
5	(0.5ℓ, 0.5ℓ, 0)	1.0948	0.1920	-0.0544
6	(ℓ, 0.5ℓ, 0)	0.3084	-0.0583	0.0260
7	(0, ℓ, 0)	-0.4276	-0.1967	-0.1966
8	(0.5ℓ, ℓ, 0)	0.3085	-0.0581	0.0266
9	(ℓ, ℓ, 0)	0.2416	-0.1283	-0.368

5.1 Example 1

Let the cube Ω, with the Poisson ratio $\nu = 0.0$, be subjected to a constant normal traction σ_0 on its face $x_3 = \ell$ (*i.e.* $\sigma_{33}(x_1, x_2, \ell) = \sigma_0$), the other faces, $x_1 = \ell$ and $x_2 = \ell$, being traction free.

The exact solution of this problem can be found in [22]: $u_3(\boldsymbol{x}) = (1 - \exp(-2\beta x_3))\sigma_0/2\beta E_0$, $u_1 = u_2 = 0$, $\sigma_{33}(\boldsymbol{x}) = \sigma_0$ and the remaining stresses vanishing, $\sigma_{ij} = 0$ for $(i,j) \neq (3,3)$.

The accuracy of the solution when refining the mesh can be observed in Tables 1 and 2 where the percentage of the normalized error in the normal stresses $\sigma_{33}(x_1, x_2, 0)$ and the displacements $u_3(\ell, \ell, x_3)$ are presented for the smaller value of the grading coefficient ($\beta = (\ln 2)/\ell$). Although the convergence is not uniform, due to the very coarse meshes used, the level of the errors is excellent. In particular, for the extremely coarse mesh A the maximum error in stresses is already about 1%, whereas mesh C provides errors less than 0.2%. Errors in displacements are even smaller, less than 0.4% for mesh A and less than 0.004% for mesh C.

The results obtained for the substantially stronger grading ($\beta = (\ln 7)/\ell$) are shown in Tables 3 and 4. Although, as could be expected, the level of error is somewhat higher than in the previous case, errors in stresses and displacements, respectively, under 0.9% and 0.5% are still excellent in view of the relatively coarse mesh B used.

Table 2: Normalized errors in u_3 along the edge $x_1 = x_2 = \ell$. Grading coefficient $\beta = (\ln 2)/\ell$. Meshes A, B and C.

		Normalized error (%)		
Node	Coordinates	A	B	C
1	$(\ell, \ell, 0.17\ell)$			0.0010
2	$(\ell, \ell, 0.25\ell)$		-0.0245	
3	$(\ell, \ell, 0.33\ell)$			0.0000
4	$(\ell, \ell, 0.50\ell)$	-0.2638	-0.0335	-0.0006
5	$(\ell, \ell, 0.67\ell)$			-0.0015
6	$(\ell, \ell, 0.75\ell)$		-0.0411	
7	$(\ell, \ell, 0.83\ell)$			-0.0029
8	(ℓ, ℓ, ℓ)	-0.3913	-0.0383	-0.0031

Table 3: Normalized errors in σ_{33} at the plane $x_3 = 0$. Grading coefficient $\beta = (\ln 7)/\ell$. Mesh B.

		Normalized error (%)
Node	Coordinates	B
1	$(0, 0, 0)$	0.0145
2	$(0.5\ell, 0, 0)$	0.8022
3	$(\ell, 0, 0)$	-0.4717
4	$(0, 0.5\ell, 0)$	0.8924
5	$(0.5\ell, 0.5\ell, 0)$	0.1422
6	$(\ell, 0.5\ell, 0)$	0.8024
7	$(0, \ell, 0)$	0.6548
8	$(0.5\ell, \ell, 0)$	0.8927
9	$(\ell, \ell, 0)$	0.0140

Table 4: Normalized errors in u_3 along the edge $x_1 = x_2 = \ell$. Grading coefficient $\beta = (\ln 7)/\ell$. Mesh B.

		Normalized error (%)
Node	Coordinates	B
1	$(\ell, \ell, 0.25)$	0.2521
2	$(\ell, \ell, 0.5\ell)$	0.4067
3	$(\ell, \ell, 0.75\ell)$	0.4452
4	(ℓ, ℓ, ℓ)	0.4462

Table 5: Normalized errors in σ_{11} along the edge $x_1 = x_2 = 0$. Grading coefficient $\beta = (\ln 2)/\ell$. Meshes A, B and C.

		Normalized error (%)		
Node	Coordinates	A	B	C
1	(0, 0, 0)	0.713307	0.090730	0.019430
2	(0, 0, 0.17ℓ)			-0.035429
3	(0, 0, 0.25ℓ)		-0.005309	
4	(0, 0, 0.33ℓ)			0.009429
5	(0, 0, 0.50ℓ)	0.023527	0.023982	-0.065233
6	(0, 0, 0.67ℓ)			-0.000443
7	(0, 0, 0.75ℓ)		-0.001453	
8	(0, 0, 0.83ℓ)			-0.105120
9	(0, 0, ℓ)	-1.093050	-0.203555	-0.085220

Table 6: Normalized errors in u_1 along the line $x_2 = 0.5\ell$ and $x_3 = \ell$. Grading coefficient $\beta = (\ln 2)/\ell$. Meshes A, B and C.

		Normalized error (%)		
Node	Coordinates	A	B	C
1	(0.5ℓ, 0.5ℓ, ℓ)	0.0639	0.0023	-0.0564
2	(ℓ, 0.5ℓ, ℓ)	0.1677	0.0215	-0.0287

5.2 Example 2

In this example, let the cube Ω be subjected to a constant normal displacement $\sigma_0\ell/E_0$ on its face $x_1 = \ell$ (*i.e.* $u_1(\ell, x_2, x_3) = \sigma_0\ell/E_0$), the other faces, $x_2 = \ell$ and $x_3 = \ell$, being traction free. In addition, the Poisson ratio is specified as $\nu = 0.3$ and the grading coefficient $\beta = (\ln 2)/\ell$.

The exact solution of this problem can also be found in [22]: $u_1(\boldsymbol{x}) = \sigma_0 x_1/E_0$, $u_2 = -\nu\sigma_0 x_2/E_0$, $u_3 = -\nu\sigma_0 x_3/E_0$, $\sigma_{11}(\boldsymbol{x}) = \sigma_0 \exp(2\beta x_3)$, with the remaining stresses vanishing, $\sigma_{ij} = 0$ for $(i, j) \neq (1, 1)$.

Tables 5, 6 and 7 present the normalized errors obtained. As in the previous example, an excellent accuracy has been obtained, although the results do not show a uniform convergence, again due to the very coarse meshes used. Spefically, the errors in the normal stresses $\sigma_{11}(0, 0, x_3)$ are less than 1.1% for mesh A and 0.11% for mesh C, errors in the displacements $u_1(x_1, 0.5\ell, \ell)$ are less than 0.17% for mesh A and 0.06% for mesh C, and errors in displacements $u_3(\ell, 0.5\ell, x_3)$ are less than 0.07% for mesh A and 0.021% for mesh C.

Table 7: Normalized errors in u_3 along the line $x_1 = \ell$ and $x_2 = 0.5\ell$. Grading coefficient $\beta = (\ln 2)/\ell$. Meshes A, B and C.

		Normalized error (%)		
Node	Coordinates	A	B	C
1	(ℓ, 0.5ℓ, 0.17ℓ)			0.0004
2	(ℓ, 0.5ℓ, 0.25ℓ)		-0.0036	
3	(ℓ, 0.5ℓ, 0.33ℓ)			0.0018
4	(ℓ, 0.5ℓ, 0.50ℓ)	-0.0567	-0.0067	0.0076
5	(ℓ, 0.5ℓ, 0.67ℓ)			0.0161
6	(ℓ, 0.5ℓ, 0.75ℓ)		-0.0063	
7	(ℓ, 0.5ℓ, 0.83ℓ)			0.0207
8	(ℓ, 0.5ℓ, ℓ)	-0.0642	-0.0117	0.0147

6 Conclusions

The numerical solution of the 3D Somigliana displacement identity for isotropic elastic exponentially graded materials by a direct collocation BEM code has been successfully developed.

First, a new expression of the strongly singular fundamental solution in tractions for such materials has been deduced. Then, the fundamental solutions in displacements, $U_{j\ell}$, and tractions, $T_{j\ell}$, have been implemented in the BEM code. To the best knowledge of the authors, this is the first implementation of a 3D direct BEM code for such materials. The numerical solution of a few examples with known analytic solutions have produced excellent accuracy, confirming the correctness of the kernel functions and their implementation.

The remaining problem to use this approach in a convenient way from now on is simply computation time: the evaluation of the Green's function kernels is quite expensive and techniques to reduce this cost must be developed. One option is to develop faster techniques for computing the kernels (*e.g.*, table look-up), and another is to implement the BEM code on a multi-processor machine.

Acknowledgements The present work has been developed during the stay of R. Criado at the Oak Ridge National Laboratory (funded by the Applied Mathematical Sciences Research Program of the Office of Mathematical, Information, and Computational Sciences, U.S. Department of Energy, under contract DE-AC05-00OR22725 with UT-Battelle), and the stays of J.E. Ortiz and L. Gray at the University of Seville (funded by the Spanish Ministry of Education, Culture and Sport; Juan de la Cierva Programm and SAB2003-0088, respectively). V. Mantič and F. París have been supported by the Spanish Ministry of Science and Technology through project MAT2003-03315.

References

[1] Suresh S, Mortensen A. *Fundamentals of Functionally Graded Materials.* IOM Communications: London, 1998.

[2] Lee Y-D, Erdogan F. Interface cracking of FGM coatings under steady-state heat flow. *Engineering Fracture Mechanics* 1998; **59** 361–380.

[3] Santare MH., Lambros J. Use of graded finite elements to model the behavior of nonhomogeneous materials. *Journal of Applied Mechanics* 2000; **67**: 819–822.

[4] Anlas G, Santare MH., Lambros J. Numerical calculation of stress intensity factors in functionally graded materials. *International Journal of Fracture* 2000; **104** 131–143.

[5] Kim J, Paulino GH. Finite element evaluation of mixed mode stress intensity factors in functionally graded materials. *International Journal for Numerical Methods in Engineering* 2002a; **53**:1903–1935.

[6] Kim J, Paulino GH. Isoparametric graded finite elements for nonhomogeneous isotropic and orthotropic materials. *Journal of Applied Mechanics* 2002b; **69**: 502–514.

[7] Paulino GH, Kim J. A new approach to compute T -stress in functionally graded materials by means of the interaction integral method. *Engineering Fracture Mechanics* 2004; **71**: 1907–1950.

[8] París F, Cañas J. *Boundary Element Method, Fundamentals and Applications.* Oxford University Press, 1997.

[9] Aliabadi MH. *The Boundary Element Method, Volume 2 Applications in Solids and Structures.* John Wiley & Sons, 2002.

[10] Shaw RP, Makris N. Green's function for Helmholtz and Laplace equations in heterogeneous media. *Engineering Analysis with Boundary Elements* 1992; **10**: 179–183.

[11] Clements D.L. Fundamental solutions for second order linear elliptic partial differential equations. *Computational Mecahnics* 1998; **22**: 26–31.

[12] Gray LJ, Kaplan T, Richardson JD, Paulino GH. Green's function and boundary integral analysis for exponentially graded materials: heat conduction. *Journal of Applied Mechanics* 2003; **40**: 543–549.

[13] Berger JR, Martin PA, Mantič V, Gray LJ. Fundamental solution for steady-state heat transfer in an exponentially graded anisotropic material. *ZAMP* 2005; **56**: 293–303.

[14] Kuo HY, Chen T. Steady and transient Greens functions for anisotropic conduction in an exponentially graded solid. *International Journal of Solids and Structures* 2005; **42** 1111-1128.

[15] Clements DL, Budhi WS, A boundary element method of the solution of a class of steady-state problems for anisotropic media. *Journal of Heat Transfer* 1999; **121**: 462–465.

[16] Núñez JP, Mantič V, París F, Berger J. Boundary element analysis of heat transfer at an interface crack in an FGM coating. *ECCM-10, Composites for the Future, 10th European Conference on Composite Materials (CD)*, Brugge, The European Society for Composite Materials (ESCM) 2002.

[17] Paulino GH, Sutradhar A, Gray LJ. Boundary Element Methods for Functionally Graded Materials. IABEM 2002 (CD), Austin, USA.

[18] Sutradhar A, and Paulino G. H., The simple boundary element method for transient heat conduction in functionally graded materials. *Computer Methods in Applied Mechanics and Engineering* 2004; **193**: 4511–4539.

[19] Chan Y, Gray LJ, Kaplan T., Paulino GH. Green's function for a two-dimensional exponentially graded elastic medium. *Proceedings Royal Society London A* 2004; **460**: 1689–1706.

[20] Martin P. A., Richardson J. D., Gray L. J. and Berger J. R. On Green's function for a three-dimensional exponentially graded elastic solid. *Proceedings Royal Society London A* 2002; **458**: 1931–1947.

[21] Criado R. Desarrollo y programación de la solución fundamental en desplazamientos y tensiones para el problema elástico tridimensional en materiales exponencialmente graduados isótropos. *Proyecto Fin de Carrera*, ETSI, Universidad de Sevilla, 2005.

[22] Criado R, Gray LJ, Mantič V, París F. Green's Function Evaluation for Three Dimensional Exponentially Graded Elasticity. *International Journal for Numerical Methods in Engineering* (submitted) 2006.

[23] Mantič V. A new formula for the C-matrix in the Somigliana identity. *Journal of Elasticity* 1993; **33**: 191–201.

[24] Lachat JC, Watson JO. Effective numerical treatment of boundary integral equations: a formulation for three-dimensional elastostatics. *International Journal for Numerical Methods in Engineering* 1976; **10** 991–1005.